



## OPEN ACCESS

## EDITED BY

Efstathios Giotis,  
University of Essex, United Kingdom

## REVIEWED BY

Chuan Wang,  
Gansu Agricultural University, China  
Krzysztof Piotr Michalak,  
Adam Mickiewicz University, Poland

## \*CORRESPONDENCE

Haiyan Zhang  
✉ 52897899@qq.com  
Jingliang Su  
✉ suzhang@cau.edu.cn

†These authors have contributed equally to this work

RECEIVED 11 November 2025

REVISED 24 December 2025

ACCEPTED 07 January 2026

PUBLISHED 09 February 2026

## CITATION

Yu Z, Chen X, Zhuo W, Ma Z, Xu Z, Liu K, Wang J, Li T, Zhu G, Wang B, Xiong R, Li C, Zhang H and Su J (2026) Disruption of cellular calcium homeostasis by duck Tembusu virus facilitates viral replication via AMPK pathway activation. *Front. Cell. Infect. Microbiol.* 16:1743907. doi: 10.3389/fcimb.2026.1743907

## COPYRIGHT

© 2026 Yu, Chen, Zhuo, Ma, Xu, Liu, Wang, Li, Zhu, Wang, Xiong, Li, Zhang and Su. This is an open-access article distributed under the terms of the [Creative Commons Attribution License \(CC BY\)](https://creativecommons.org/licenses/by/4.0/). The use, distribution or reproduction in other forums is permitted, provided the original author(s) and the copyright owner(s) are credited and that the original publication in this journal is cited, in accordance with accepted academic practice. No use, distribution or reproduction is permitted which does not comply with these terms.

# Disruption of cellular calcium homeostasis by duck Tembusu virus facilitates viral replication via AMPK pathway activation

Ziding Yu<sup>1,2†</sup>, Xiaoyong Chen<sup>3,4†</sup>, Wenxiao Zhuo<sup>1,2</sup>, Zhenxing Ma<sup>1,2</sup>, Zejun Xu<sup>1,2</sup>, Kuanhui Liu<sup>1,2</sup>, Julong Wang<sup>1,2</sup>, Ting Li<sup>1,2</sup>, Guangshuang Zhu<sup>1,2</sup>, Benzhong Wang<sup>1,2</sup>, Ran Xiong<sup>1,2</sup>, Chao Li<sup>1,2</sup>, Haiyan Zhang<sup>1,2\*</sup> and Jingliang Su<sup>5\*</sup>

<sup>1</sup>Wuhu Vocational Technical University, Wuhu, China, <sup>2</sup>Detection of Food-borne Pathogenic Microorganisms Engineering Research Center of Wuhu, Wuhu, China, <sup>3</sup>Xingzhi College, Zhejiang Normal University, Jinhua, China, <sup>4</sup>College of Life Sciences, Zhejiang Normal University, Jinhua, China, <sup>5</sup>Key Laboratory of Animal Epidemiology and Zoonosis, Ministry of Agriculture, College of Veterinary Medicine, China Agricultural University, Beijing, China

**Background:** The flavivirus Duck Tembusu virus (DTMUV) exhibits high pathogenicity and transmissibility, posing a severe threat to the poultry industry in China and Southeast Asia. Although the molecular mechanisms of DTMUV pathogenesis remain unclear, its potential to disrupt intracellular calcium ion (Ca<sup>2+</sup>) homeostasis, a known driver of viral replication, has not been investigated. Here, we investigated the role and underlying mechanism of Ca<sup>2+</sup> homeostasis in DTMUV infection.

**Methods:** Fluo-4AM staining and flow cytometry of duck embryo fibroblasts (DEFs) were used to detect cytoplasmic Ca<sup>2+</sup>. To modulate Ca<sup>2+</sup> levels and AMP-activated protein kinase (AMPK) activity, we used voltage-gated calcium channel (VGCC) blockers (verapamil, diltiazem hydrochloride), a Ca<sup>2+</sup> chelator (BAPTA-AM), and an AMPK inhibitor (Compound C). Viral entry, genomic RNA replication (targeting the DTMUV NS5 gene), viral yield, and release were evaluated via qRT-PCR and plaque assays. AMPK activation was detected using western blotting with anti-phospho-AMPK $\alpha$  (Thr172) and anti-AMPK $\alpha$  antibodies. Statistical analyses were performed using Student's t-test or two-way analysis of variance.

**Results:** DTMUV infection significantly increased cytoplasmic Ca<sup>2+</sup> in DEFs at 6, 8, 10, and 12 hours post-infection. This elevation was suppressed by treatment with verapamil or diltiazem hydrochloride, indicating that DTMUV induces extracellular Ca<sup>2+</sup> influx via VGCCs. Functional assays showed that reducing cytoplasmic Ca<sup>2+</sup> via treatment with VGCC blockers or BAPTA-AM specifically inhibited DTMUV RNA replication, but not viral entry or release, decreasing progeny virus production. Further mechanistic analysis revealed that DTMUV infection activates the AMPK pathway in a Ca<sup>2+</sup>-dependent manner, with Compound C-mediated AMPK inhibition dose-dependently suppressing viral RNA replication and progeny yield.

**Conclusions:** DTMUV disrupts host  $\text{Ca}^{2+}$  homeostasis to activate AMPK, which promotes viral RNA replication. This study provides novel insights into DTMUV pathogenesis and identifies  $\text{Ca}^{2+}$ –AMPK signaling as a potential anti-DTMUV target.

#### KEYWORDS

AMPK, antiviral target,  $\text{Ca}^{2+}$  homeostasis, DTMUV, VGCCs, viral RNA replication

## 1 Introduction

Duck Tembusu virus (DTMUV) is an enveloped, single-stranded positive-sense RNA virus belonging to the genus *Flavivirus* within the family *Flaviviridae*. The genome of DTMUV is approximately 11,000 nucleotides (nt) in length, containing one open reading frame (ORF) that encodes three structural proteins (C, PrM, E) and seven non-structural (NS) proteins (NS1, NS2A, NS2B, NS3, NS4A, NS4B, and NS5) (Tang et al., 2012). The Tembusu virus (TMUV) prototype strain MM1775 was first isolated from mosquitoes in 1955 (Platt et al., 2016). In 2010, a DTMUV outbreak occurred in southeastern China, characterized by encephalitis and a sharp decline in egg production in duck and goose flocks (Qiu et al., 2011). Subsequently, diseases associated with this virus were also reported in Southeast Asian countries (Homonnay et al., 2014; Ninvilai et al., 2018). In recent years, accumulating studies have confirmed that several DTMUV strains, characterized by substantial antigenic variation and belonging to a unique genetic cluster, have begun circulating in chicken flocks (Yu et al., 2021; Yan et al., 2022). DTMUV exhibits high pathogenicity and transmissibility, with infection in avian hosts leading to a marked decline in egg production and triggering neurological symptoms, typically encephalitis. Currently, this virus is widely distributed across China and Southeast Asia, causing enormous economic losses to the regional poultry industry. Although vaccination has historically been a key strategy for DTMUV control, effective prevention requires elucidating its pathogenic mechanisms to identify potential antiviral targets.

The calcium ion ( $\text{Ca}^{2+}$ ) is one of the most ubiquitous and versatile signaling molecules in eukaryotic cells. As an intracellular second messenger,  $\text{Ca}^{2+}$  is involved in regulating almost all cellular physiological processes, including gene transcription, differentiation, proliferation, and kinase activation (Berridge et al., 2000, 2003). Under normal cellular physiology, intracellular  $\text{Ca}^{2+}$  homeostasis—maintaining stable cytoplasmic  $\text{Ca}^{2+}$  concentrations—is tightly regulated by the coordinated interplay of channels, transporters, and pumps (Berridge et al., 2003). As a stimulant, viruses often disrupt intracellular  $\text{Ca}^{2+}$  homeostasis by hijacking  $\text{Ca}^{2+}$ -mediated signaling transduction pathways to facilitate the infection cycle. For instance, upon infecting host cells, duck enteritis virus (DEV) and porcine reproductive and respiratory syndrome virus (PRRSV) increase cytoplasmic  $\text{Ca}^{2+}$  concentrations,

inducing autophagy mediated by the calmodulin-dependent protein kinase II (CaMKK-II) and adenosine 5'-monophosphate-activated protein kinase (AMPK) pathway to promote their own replication (Yin et al., 2018; Manicassamy et al., 2023). Within the genus *Flavivirus*, host cell infection by West Nile virus (WNV) and dengue virus (DENV) also induces an increase in cytoplasmic  $\text{Ca}^{2+}$  concentration. Importantly, pharmacological inhibition of this  $\text{Ca}^{2+}$  elevation significantly reduces the production of viral particles, suggesting that the infection-induced elevation in cytoplasmic  $\text{Ca}^{2+}$  is essential for the replication of these flaviviruses (Scherbik and Brinton, 2010; Dionicio et al., 2018).

Despite the well-documented association between  $\text{Ca}^{2+}$  homeostasis and flavivirus infection, its role in DTMUV infection remains uncharacterized. Here, we report the first investigation of this association, demonstrating that DTMUV infection significantly increases cytoplasmic  $\text{Ca}^{2+}$  concentrations in host cells. Furthermore, this elevation in  $\text{Ca}^{2+}$  activates the AMPK signaling pathway, a critical mediator of DTMUV RNA replication. These findings lay a solid foundation for elucidating the molecular mechanisms of DTMUV pathogenesis and offer new insights into potential targets for anti-DTMUV strategies.

## 2 Materials and methods

### 2.1 Cell culture and virus

Baby hamster kidney (BHK)-21 cells were obtained from the American Type Culture Collection (Manassas, VA, USA). Duck embryo fibroblasts (DEFs) were prepared from 10-day-old duck embryos obtained from Shandong Health-Tech Laboratory Animal Breeding Co., Ltd. (Jinan, China) following standard procedures. DEFs cells were cultured in Dulbecco's modified Eagle's medium (DMEM) containing 10% fetal bovine serum (FBS) and 1% penicillin-streptomycin at 37 °C with 5%  $\text{CO}_2$ . DTMUV strain JXSP was isolated and preserved in our laboratory.

### 2.2 Drug treatment and virus infection

The calcium channel blockers verapamil (Cat# HY-14275) and diltiazem hydrochloride (Cat# HY-14656), the AMPK inhibitor

Compound C (Cat# HY-13418A), and calcium chelating agent BAPTA-AM (Cat# HY-100545) were purchased from MedChemExpress (Monmouth Junction, NJ, USA). All drugs were dissolved and stored in DMSO according to manufacturer instructions. Prior to use, each drug was diluted to its final working concentration in DMEM containing 1% FBS and 1% penicillin-streptomycin: verapamil (25  $\mu$ M), diltiazem hydrochloride (50  $\mu$ M), BAPTA-A (25  $\mu$ M), and Compound C (2.5  $\mu$ M or 5  $\mu$ M). For drug treatment and virus infection, DEFs grown in 6-well plates or 12-well plates were washed thrice with sterile phosphate-buffered saline (PBS), then inoculated with DTMUV (multiplicity of infection [MOI] = 1) concurrent with the corresponding drug treatment. After 1 hour, the supernatant was replaced with fresh drug-containing DMEM. Cells and supernatants were collected at the indicated time points for reverse transcription quantitative real-time PCR (RT-qPCR), western blotting, or virus titration analysis.

To assay viral entry, DEFs cultured in 6-well plates were washed thrice with sterile PBS and pretreated with diltiazem hydrochloride (50  $\mu$ M) and BAPTA-AM (25  $\mu$ M) for 1 hour. After another three washes with sterile PBS, cells were infected with DTMUV (MOI = 1) at 4°C for 1 hour to allow viral attachment while blocking fusion. After a wash to remove unbound virus, cells were shifted to 37°C for 1 hour to initiate fusion. Viral RNA levels in the cytoplasm were quantified by RT-qPCR at 2 hours post-infection (hpi).

To assay viral replication, DEFs cultured in 6-well plates were washed thrice with sterile PBS and incubated with DTMUV for 2 hours. The supernatants were removed, and the cells were cultured in fresh medium containing diltiazem hydrochloride (50  $\mu$ M) or BAPTA-AM (25  $\mu$ M). At 6 hpi, the infected cells were collected and expression of the DTMUV NS5 gene was quantified by RT-qPCR.

To assay viral release, DEFs cultured in 6-well plates were washed thrice with sterile PBS and incubated with DTMUV. At 10 hpi, the supernatants were replaced with fresh medium containing diltiazem hydrochloride (50  $\mu$ M) or BAPTA-AM (25  $\mu$ M). Two hours later, the cell supernatants were harvested and titrated by plaque assay.

#### Plaque assay.

Cell supernatant samples were serially diluted 10-fold with DMEM containing 2% FBS and 1% penicillin-streptomycin. Each dilution was used to inoculate a monolayer of BHK-21 cells in 12-well plates (1 mL/well), followed by incubation at 37°C for 1 hour with gentle rocking every 15 min. After removing the inoculum, cells were washed thrice with sterile PBS and overlaid with DMEM containing 1% (wt/vol) low-melting-point agar (Amresco, Spokane, WA, USA), 2% FBS, and 1% penicillin-streptomycin. Following overlay solidification at 4°C, the plates were incubated at 37°C for 3 days. Plaques were visualized and counted following staining of viable cells with neutral red (0.02%).

## 2.3 Viral RNA extraction and RT-qPCR

Total RNA of virus-infected DEFs was extracted using TRIzol reagent. The cDNA was synthesized using random primers and a reverse transcription system (Promega, Madison, WI, USA), in accordance with the manufacturer's instructions. RT-qPCR was

performed on a Bio-Rad CFX Connect instrument using the SYBR green SuperReal PreMix Plus kit (Tiangen, Beijing, China) and the following JXSP NS5-specific primers: forward, 5'-TTGGGACACCTTGCAAAACG-3'; reverse, 5'-TTGCCACGATGTTTCATGACC-3', and duck GAPDH-specific primers: forward, 5'-AAATTGTCAGCAATGCCTCTTG-3'; reverse, 5'-TGGCATGGACAGTGGTCATAA-3'. The 20- $\mu$ L reaction mixture comprised 10  $\mu$ L SuperReal PreMix Plus, 0.3  $\mu$ L of specific primers, 7.7  $\mu$ L sterile double-distilled water and 2  $\mu$ L of cDNA template. The cycling conditions were as follows: initial denaturation at 95°C for 15 min; and 40 cycles of denaturation at 95°C for 10 s and annealing/extension at 60°C for 30 s. GAPDH was used as the reference housekeeping gene for internal standardization. The data of quantitative real-time PCR analysis were shown in normalized ratios and auto-calculated using  $\Delta\Delta$ CT method.

## 2.4 Measurement of cytoplasmic Ca<sup>2+</sup> concentration

Cytoplasmic Ca<sup>2+</sup> concentrations were measured using Fluo-4AM (Beyotime, Shanghai, China) and flow cytometry. Briefly, DEFs infected with DTMUV at different time points or treated with different drugs were rinsed three times with sterile PBS, followed by staining with Fluo-4AM (diluted to 5  $\mu$ M in sterile PBS) at 37°C for 1 h and another three rinses. The cells were then detached via trypsinization, filtered through a 40- $\mu$ m cell strainer (Beyotime, Shanghai, China) to prepare a single-cell suspension, and analyzed on a LSR II flow cytometer (BD Biosciences). The mean fluorescence intensity (MFI) analysis was performed using FlowJo software (Version 10.8.1, BD Biosciences, San Jose, CA, USA) according to the following standardized protocol. Raw FCS files of the samples were imported into FlowJo. Cell debris and doublets were excluded by gating to retain target cells, with consistent gating applied across all samples. For each assay, 10,000 target cells were collected within this gate. In the FITC channel, the MFI of the gated target population was quantified using the built-in Mean function of FlowJo for Fluo-4AM-stained samples. Statistical analysis of the measured MFI values was conducted using GraphPad Prism 8 (see Data Analysis).

## 2.5 Western blotting

DEFs were lysed using cell lysis buffer containing 1% phenylmethanesulfonyl fluoride (Beyotime), following the manufacturer's protocol. Cell fragments were removed by low-temperature centrifugation (4°C, 12,000  $\times$  g, 10 min). The resulting supernatant was thoroughly mixed with 6 $\times$  sodium dodecyl sulfate-polyacrylamide gel electrophoresis (SDS-PAGE) sample loading buffer (Beyotime), boiled for 5 min, separated by SDS-PAGE, and transferred onto a formaldehyde-activated polyvinylidene fluoride (PVDF) membrane. The PVDF membrane was blocked with 5% skim milk and probed with the following antibodies: anti-phospho-AMPK $\alpha$  (Thr172) antibody (Cell Signaling Technology, Beverly, MA, USA), to assess AMPK

activation levels; anti-AMPK $\alpha$  antibody (Cell Signaling Technology), to measure total AMPK protein expression; and anti- $\beta$ -actin antibody (Beyotime), as a control for sample consistency.

## 2.6 Data analysis

Data were processed using GraphPad Prism 8 (GraphPad Software Inc., La Jolla, CA, USA). Statistical comparisons between two groups were performed using Student's t-test (for two-group comparisons) or one-way/two-way analysis of variance (ANOVA) with multiple comparisons, as appropriate. A  $p$  value  $< 0.05$  was considered statistically significant.

## 3 Results

### 3.1 DTMUV infection disrupts cytoplasmic $\text{Ca}^{2+}$ homeostasis by inducing extracellular $\text{Ca}^{2+}$ influx through voltage-gated calcium channels

Mounting evidence from virology studies has established that many viral pathogens disrupt intracellular  $\text{Ca}^{2+}$  homeostasis to create a favorable microenvironment for their propagation. To determine whether DTMUV infection affects this process, we monitored cytoplasmic  $\text{Ca}^{2+}$  concentrations throughout the infection cycle. Cytoplasmic  $\text{Ca}^{2+}$  levels were quantified by flow cytometry as MFI following staining with Fluo-4AM, a  $\text{Ca}^{2+}$ -specific fluorescent probe. As illustrated in Figures 1A and B, intracellular  $\text{Ca}^{2+}$  levels of DEFs significantly increased at 6, 8, 10, and 12 hpi. This elevation was significantly inhibited by concurrent treatment with VGCC blockers (verapamil or diltiazem hydrochloride) (Figure 1C), indicating that DTMUV-induced cytoplasmic  $\text{Ca}^{2+}$  influx is primarily mediated through VGCCs. Collectively, these findings demonstrated that DTMUV infection disrupts  $\text{Ca}^{2+}$  homeostasis in host cells.

### 3.2 Cytoplasmic $\text{Ca}^{2+}$ is an essential regulator of DTMUV production in DEFs

Given the functional link between viral-induced dysregulation of  $\text{Ca}^{2+}$  homeostasis and viral replication, we sought to determine whether the DTMUV-mediated elevation in cytoplasmic  $\text{Ca}^{2+}$  contributes to viral propagation. Verapamil and diltiazem hydrochloride were initially employed to inhibit extracellular  $\text{Ca}^{2+}$  influx and reduce cytoplasmic  $\text{Ca}^{2+}$  levels, followed by measurement of progeny virus production. Both VGCC blockers significantly reduced the number of progeny virus particles in DEFs with diltiazem hydrochloride exhibiting the most pronounced inhibitory effect (Figure 2A). Additionally, we evaluated DTMUV production in the presence of the cytoplasmic  $\text{Ca}^{2+}$  chelator BAPTA-AM. As shown in Figure 2B, replication of DTMUV in DEFs was markedly diminished

when either extracellular or cytoplasmic  $\text{Ca}^{2+}$  was chelated. These findings indicated that DTMUV promotes its replication by elevating cytoplasmic  $\text{Ca}^{2+}$  levels.

### 3.3 Reducing cytoplasmic $\text{Ca}^{2+}$ inhibits the replication step of DTMUV infection

To further delineate the specific step(s) in the DTMUV life cycle that are regulated by cytoplasmic  $\text{Ca}^{2+}$ , we performed a series of stage-specific functional assays of viral entry, viral RNA replication, and viral release.

For the viral entry assay (Figure 3A), DEFs were pretreated with diltiazem hydrochloride or BAPTA-AM prior to a brief DTMUV attachment and entry period. Intracellular viral RNA was quantified by RT-qPCR after removal of unbound virus. No significant difference was observed between the treated and untreated groups, indicating that reducing cytoplasmic  $\text{Ca}^{2+}$  does not affect the DTMUV entry step.

For the viral RNA replication assay (Figure 3B), DEFs were first infected with DTMUV to allow efficient viral entry, then treated with diltiazem hydrochloride or BAPTA-AM following the removal of unbound virus. At specified time points, intracellular viral RNA was quantified by RT-qPCR. In contrast to the viral entry results, reducing cytoplasmic  $\text{Ca}^{2+}$  levels with either drug significantly inhibited the accumulation of DTMUV genomic RNA, demonstrating a direct effect on viral RNA replication.

To assess viral release, DEFs were infected with DTMUV and treated with diltiazem hydrochloride or BAPTA-AM at 10 hpi. At 12 hpi, viral titers in the cell culture supernatant were quantified using plaque assay. As shown in Figure 3C, there was no significant difference in the ratio of released virus to intracellular virus between treated and untreated groups ( $p > 0.05$ ), demonstrating that cytosolic  $\text{Ca}^{2+}$  reduction does not impact DTMUV release.

To validate the reproducibility and generalizability of these findings, we further investigated the effects of verapamil, diltiazem hydrochloride, and BAPTA-AM on DTMUV RNA replication throughout the infection cycle in DEFs and assessed their impact on DTMUV genomic RNA replication. Consistently, all three drugs also significantly inhibited the replication of DTMUV genomic RNA in these cells throughout the infection cycle (Figure 3D).

Collectively, these data demonstrated that reducing cytosolic  $\text{Ca}^{2+}$  levels specifically impairs the viral RNA replication step of the DTMUV life cycle.

### 3.4 Cytosolic $\text{Ca}^{2+}$ promotes DTMUV replication by activating the AMPK pathway

Elevated cytosolic  $\text{Ca}^{2+}$  acts as a universal intracellular signal transducer regulating diverse cellular processes in eukaryotes, including activation of the AMPK pathway, a central regulator of energy homeostasis (Tokumitsu and Sakagami, 2022; Herzig and Shaw, 2017). Several viruses have been shown to actively exploit

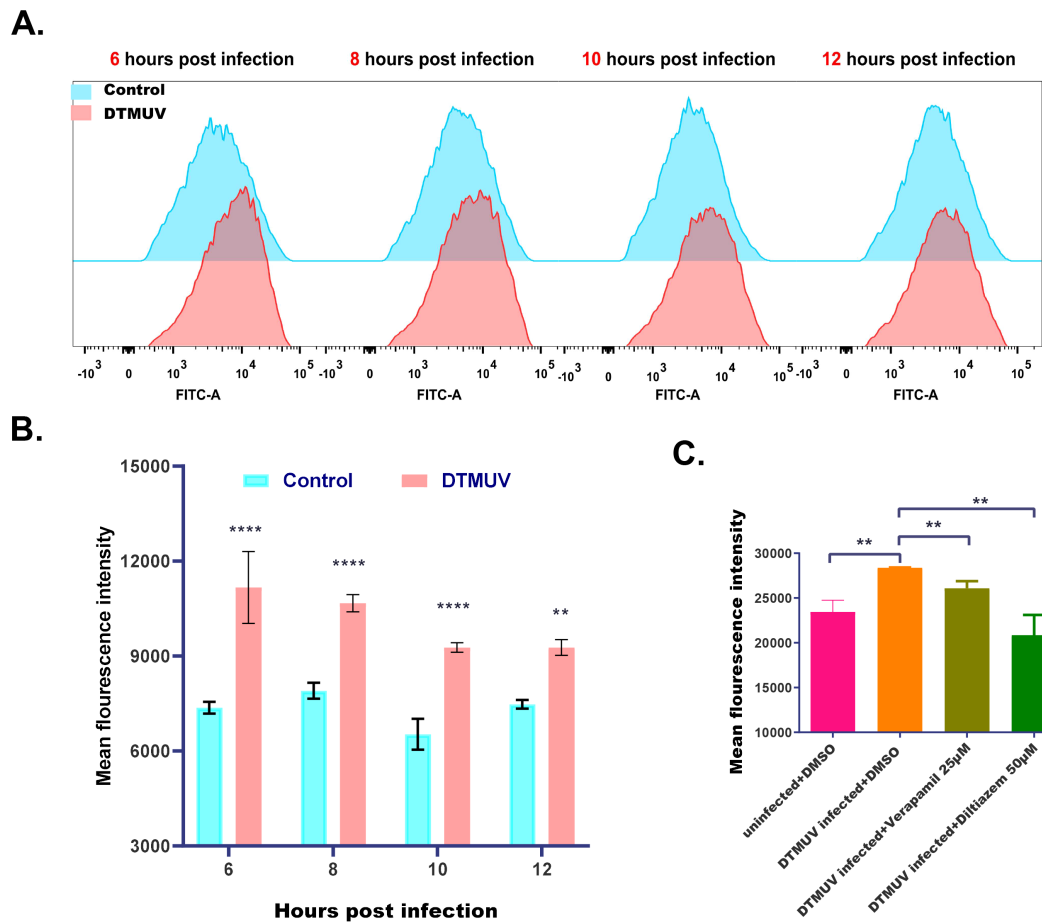


**FIGURE 1** DTMUV infection increases cytoplasmic Ca<sup>2+</sup> levels in DEFs. **(A)** Flow cytometry profiles showing cytoplasmic Ca<sup>2+</sup> levels in DEFs with and without DTMUV infection and probed with Flou-4AM. **(B)** Cytoplasmic Ca<sup>2+</sup> levels of DEFs with (red) and without (blue) DTMUV infection (MOI = 0.1) for 6, 8, 10, or 12 hours, expressed as mean fluorescence intensity (MFI). **(C)** Cytoplasmic Ca<sup>2+</sup> levels of DEFs with and without DTMUV infection and concurrent treatment with DMSO (control) verapamil or diltiazem hydrochloride. Data expressed as mean ± standard deviation (n = 3), analyzed using Student’s t-test; \*p < 0.05, \*\*p < 0.01, \*\*\*\*p < 0.0001.

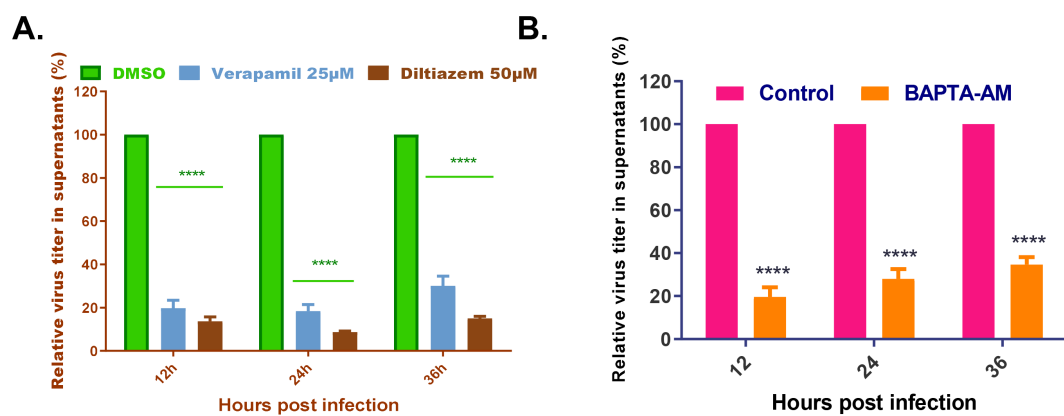


**FIGURE 2** VDCC blockers and a cytoplasmic Ca<sup>2+</sup> chelator reduce DTMUV particle production. **(A, B)** Analysis of plaque assays of DEFs infected with DTMUV and treated with verapamil (25 µM), diltiazem hydrochloride (50 µM), or DMSO (control; **(A)**), and BAPTA-AM (25 µM) or DMSO (control; **(B)**). Results expressed as the viral titer ratio (%) between each drug-treated group and the control group at 12, 24, and 36 hpi. Data expressed as mean ± standard deviation of triplicate samples, analyzed by two-way ANOVA with multiple comparisons. \*p < 0.05, \*\*p < 0.01, \*\*\*p < 0.001, \*\*\*\*p < 0.0001. Results shown are representative of three independent experiments.

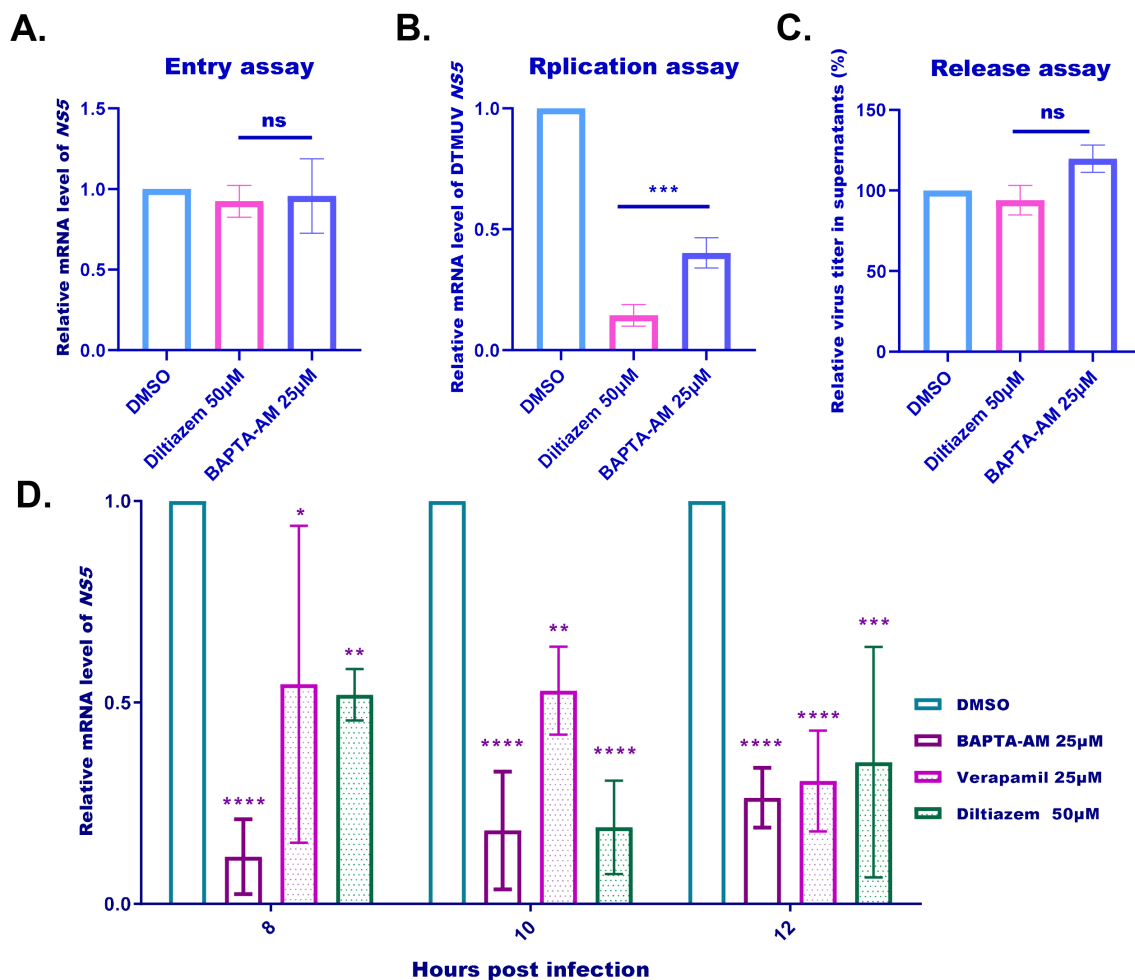


FIGURE 3

VDCC blockers and a cytoplasmic  $\text{Ca}^{2+}$  chelator inhibit the replication step of DTMUV infection. (A) Viral entry assay of DEFs pretreated with DMSO, diltiazem (50  $\mu\text{M}$ ), or BAPTA-AM (25  $\mu\text{M}$ ) for 1 hour prior to DTMUV infection (MOI = 1) at 4°C for 1 hour and fusion at 37°C. Viral RNA levels in the cytoplasm were quantified by RT-qPCR at 2 hours post-infection (hpi), expressed as relative DTMUV mRNA levels between the drug-treated groups and the control group. (B) Viral replication assay of DEFs infected with DTMUV (MOI = 1) prior to treatment with DMSO (control), diltiazem hydrochloride (50  $\mu\text{M}$ ), or EAPTA-AM (25  $\mu\text{M}$ ) at 2 hpi, and RT-qPCR analysis of viral RNA replication in infected cells at 6 hpi, expressed as relative DTMUV mRNA levels between the drug-treated and control groups. (C) Plaque assay of viral release in DEFs cultured infected with DTMUV (MOI = 1) prior to treatment with DMSO (control), diltiazem hydrochloride (50  $\mu\text{M}$ ), or EAPTA-AM (25  $\mu\text{M}$ ) at 10 hpi and plating at 12 hpi. Results expressed as the viral titer ratio (%) between the drug-treated groups and the control group. (D) Viral replication assay of DEFs infected with DTMUV (MOI = 1) prior to treatment with DMSO (control) or alternative forms of verapamil (25  $\mu\text{M}$ ), diltiazem hydrochloride (50  $\mu\text{M}$ ), or BAPTA-AM (25  $\mu\text{M}$ ) at 1 hpi. Infected cells were harvested for RT-qPCR analysis of DTMUV mRNA levels at 8, 10, and 12 hpi, expressed as relative DTMUV mRNA levels between the drug-treated and control groups. Data expressed as mean  $\pm$  standard deviation of triplicate samples, analyzed by one-way or two-way ANOVA with multiple comparisons; \* $p < 0.05$ , \*\* $p < 0.01$ , \*\*\* $p < 0.001$ , \*\*\*\* $p < 0.0001$ . Data shown are representative of three independent experiments. ns: no significant difference.

AMPK signaling to modulate their own life cycles, highlighting the critical role of this pathway in viral replication and pathogenesis (Gu et al., 2016; Yin et al., 2018; Zhang et al., 2023). Based on these observations, we hypothesized that intracellular  $\text{Ca}^{2+}$  promotes DTMUV replication via AMPK pathway activation.

To evaluate this, we first investigated the dynamic activation status of AMPK in DEFs following DTMUV infection. Compared with the non-infected group, AMPK activation was markedly enhanced at 6, 8, 10, and 12 hpi, as evidenced by a significant rise in phosphorylated (p)AMPK levels (Figure 4A). This finding confirmed that DTMUV infection induces AMPK pathway activation in DEFs.

Next, to determine whether DTMUV-mediated activation of AMPK signaling depends on cytosolic  $\text{Ca}^{2+}$  elevation, we treated cells with verapamil, diltiazem hydrochloride, or BAPTA-AM and observed significant suppression of AMPK activation with all three drugs (Figure 4B). These results clearly demonstrated that DTMUV infection induces AMPK activation in DEFs in a cytosolic  $\text{Ca}^{2+}$ -dependent manner.

To confirm that cytoplasmic  $\text{Ca}^{2+}$  promotes DTMUV replication through AMPK activation specifically, we treated infected DEFs with Compound C to pharmacologically suppress AMPK signaling. Western blot analysis verified that treatment with 2.5  $\mu\text{M}$  or 5  $\mu\text{M}$  Compound C dose-dependently reduced DTMUV-

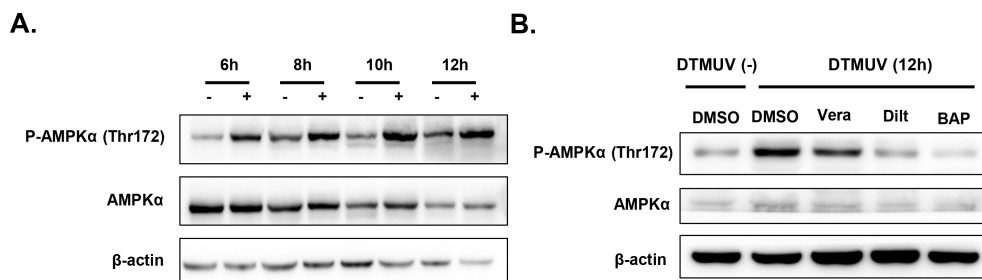


**FIGURE 4** DTMUV-mediated AMPK activation is markedly diminished by treatment with VDCC blockers or a cytoplasmic Ca<sup>2+</sup> chelator. **(A)** Western blotting of pAMPKα (Thr172) in DEFs infected with DTMUV (MOI = 1) and harvested at the indicated time points. **(B)** Immunoblotting analysis of pAMPKα (Thr172) levels in DEFs treated with DMSO (control), verapamil (25 μM; Vera), diltiazem hydrochloride (50 μM; Dilt), or BAPTA-AM (25 μM; BAP), with and without DTMUV infection (MOI = 1) for 12 hours.

induced p-AMPKα levels without affecting total AMPKα (Figure 5A). Next, we assessed the impact of AMPK inhibition on DTMUV infection by quantifying both progeny virus production (Figure 5B) and viral RNA replication (Figure 5C). Compound C-mediated inhibition of DTMUV-induced AMPK activation significantly reduced both the yield of progeny virus particles and the accumulation of DTMUV genomic RNA in a dose-dependent manner.

### 4 Discussion

As a ubiquitous intracellular second messenger, Ca<sup>2+</sup> plays a pivotal regulatory role in virtually all cellular processes throughout the cell cycle (Zhou et al., 2009). A growing body of evidence points to the active involvement of Ca<sup>2+</sup> and Ca<sup>2+</sup>-related proteins in the viral life cycle, playing a critical role in viral pathogenesis (Casciano and Bouchard, 2018; Fujioka et al., 2018; Gu et al., 2016;

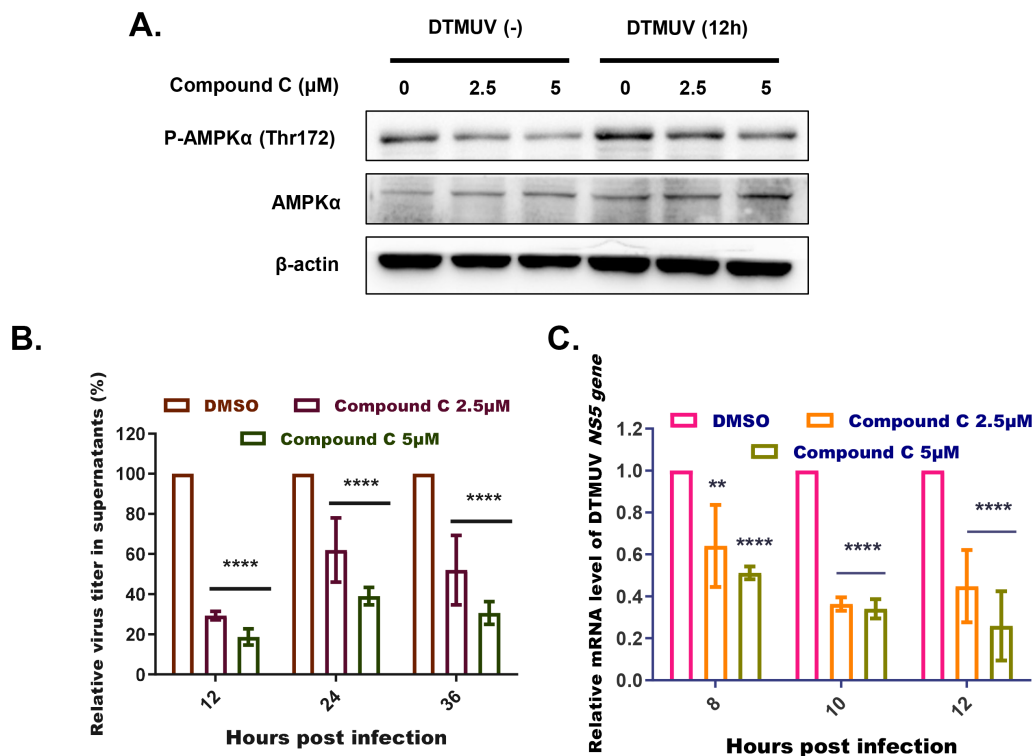


**FIGURE 5** Inhibition of AMPK activation significantly reduces DTMUV replication. **(A)** Immunoblotting analysis of pAMPKα (Thr172) levels in DEFs treated with Compound C at a range of concentrations, with or without DTMUV infection (MOI = 1) for the indicated times. **(B)** Plaque assay of DTMUV production at 12, 24, and 36 hours post infection (hpi) in DEFs treated with DMSO (control) or Compound C (2.5 μM or 5 μM), expressed as the viral titer ratio (%) between the inhibitor-treated group and the control group. **(C)** RT-qPCR analysis of relative DTMUV mRNA levels at 8, 10, and 12 hpi in DEFs treated with Compound C (2.5 or 5 μM), expressed as the viral titer ratio (%) between the inhibitor-treated group and the control group. Data expressed as means ± standard deviation of triplicate samples, analyzed by two-way ANOVA with multiple comparisons; \*\*p < 0.01, \*\*\*\*p < 0.0001. Results shown are representative of three independent experiments. ns: no significant difference.

Lee et al., 2024). In this study, we found that DTMUV infection disrupts  $\text{Ca}^{2+}$  homeostasis in host cells by increasing cytoplasmic  $\text{Ca}^{2+}$  levels. This elevation in cytoplasmic  $\text{Ca}^{2+}$  activates the AMPK pathway, promoting viral RNA replication and proliferation. To our knowledge, this is the first report linking  $\text{Ca}^{2+}$ , the AMPK pathway, and DTMUV replication.

Under normal cellular physiological conditions, intracellular  $\text{Ca}^{2+}$  homeostasis—defined as the maintenance of a stable concentration of cytoplasmic free  $\text{Ca}^{2+}$ —is tightly regulated by the coordinated interplay of multiple membrane transporters and regulatory proteins. These key mediators include plasma membrane-localized  $\text{Ca}^{2+}$  channels,  $\text{Na}^+$ - $\text{Ca}^{2+}$  exchangers, plasma membrane  $\text{Ca}^{2+}$ -ATPases; mitochondrial  $\text{Ca}^{2+}$ - $\text{H}^+$  exchangers, and a repertoire of cytoplasmic  $\text{Ca}^{2+}$ -binding proteins that act as  $\text{Ca}^{2+}$  buffers, fine-tuning cytoplasmic  $\text{Ca}^{2+}$  dynamics (Berridge et al., 2003). Viral infection, as an external stimulus, frequently disrupts intracellular  $\text{Ca}^{2+}$  homeostasis. RNA viruses such as HIV type 1, human T-lymphotropic virus type 1 (Ding et al., 2002), and hepatitis C virus (HCV) (Griffin et al., 2002), as well as DNA viruses including hepatitis B virus (Casciano and Bouchard, 2018) and herpes simplex virus types 1 and 2 (Cheshenko et al., 2003), have been shown to elevate cytosolic  $\text{Ca}^{2+}$  levels and perturb cellular  $\text{Ca}^{2+}$  homeostasis. This disruption is typically mediated by specific viral proteins that either facilitate the influx of extracellular  $\text{Ca}^{2+}$  into cells or induce the release of  $\text{Ca}^{2+}$  from intracellular stores. In this study, we found that VDCC blockers could significantly inhibit the increase in cytoplasmic  $\text{Ca}^{2+}$  concentration induced by DTMUV infection, but failed to completely abolish this effect. These results indicate that VDCCs are not the sole pathway mediating the elevation of cytoplasmic  $\text{Ca}^{2+}$  levels in DEFs upon DTMUV infection. Recent studies have reported distinct mechanisms of  $\text{Ca}^{2+}$  homeostasis disruption by closely related flaviviruses. For instance, WNV induces an influx of extracellular  $\text{Ca}^{2+}$  into infected cells by activating plasma membrane calcium channels (Scherbik and Brinton, 2010). In contrast, DENV disrupts intracellular  $\text{Ca}^{2+}$  homeostasis through two mechanistically distinct pathways: enhancement of plasma membrane permeability to  $\text{Ca}^{2+}$  and activation of the store-operated calcium entry (SOCE) pathway, which is governed by intracellular calcium stores (Dionicio et al., 2018). The aforementioned studies have demonstrated that in flavivirus-infected cellular models, both extracellular calcium influx and the release of calcium from intracellular stores disrupt cytoplasmic calcium homeostasis, resulting in elevated cytoplasmic  $\text{Ca}^{2+}$  concentrations. Therefore, it is reasonable to hypothesize that, beyond the VDCCs-mediated  $\text{Ca}^{2+}$  influx demonstrated in the present study, DTMUV infection may also trigger the release of  $\text{Ca}^{2+}$  from intracellular calcium stores via activating channels such as inositol 1,4,5-triphosphate receptors ( $\text{IP}_3\text{R}$ ) and ryanodine receptors (RyR) on the mitochondrial membrane, thereby elevating the cytoplasmic  $\text{Ca}^{2+}$  level. Further investigation is warranted to clarify these mechanisms in greater detail.

Additionally, it remains unclear how DTMUV infection activates L-type calcium channels on the plasma membrane. One possibility involves lipid rafts, which are cholesterol- and sphingolipid-rich microdomains that serve as unique signal transduction platforms. Multiple studies have demonstrated that lipid rafts and caveolar microdomains of the plasma membrane are enriched in proteins that regulate calcium signaling, including those that facilitate L-type calcium channel activation and calcium influx (Pani and Singh, 2009; Balijepalli et al., 2006). Furthermore, these lipid rafts are critically involved in the cellular entry of certain flaviviruses, including DENV and WNV (Osuna-Ramos et al., 2018). As a member of the Flavivirus genus, DTMUV is hypothesized to utilize lipid raft microdomains of the plasma membrane as a functional platform for aggregating key signaling molecules, thereby activating L-type calcium channels and mediating  $\text{Ca}^{2+}$  influx. Based on this proposed regulatory mechanism, subsequent studies should prioritize systematic, in-depth investigations to elucidate its molecular basis.

Current evidence suggests that  $\text{Ca}^{2+}$  plays a critical role in nearly every stage of the viral life cycle. Here, we demonstrated that the L-type calcium channel blocker diltiazem hydrochloride and the cytoplasmic calcium chelator BAPTA-AM reduce DTMUV yield by inhibiting the viral RNA replication step, without affecting viral entry or release. In previous studies on the interaction between cellular  $\text{Ca}^{2+}$  and viruses, pharmacologically reducing intracellular  $\text{Ca}^{2+}$  concentrations using calcium channel blockers or calcium chelators effectively inhibited viral RNA replication in Zika virus (ZIKV) (Bezemer et al., 2022), PRRSV (Manicassamy et al., 2023), porcine deltacoronavirus (PDCoV) (Bai et al., 2020), and respiratory syncytial virus (RSV) (Chen et al., 2024). Such findings are highly consistent with those of the present study. Within the  $\text{Ca}^{2+}$ -mediated intracellular signal transduction network, AMPK is activated by CaMKK-II and functions as a key intracellular energy sensor, regulating critical physiological processes including cellular metabolism and autophagy (Salt et al., 2024; Herzig and Shaw, 2017). Therefore, from a mechanistic perspective, this study focused on AMPK as a central target for investigation. Our results revealed a coupling between the DTMUV infection-induced elevation of cytoplasmic  $\text{Ca}^{2+}$  and AMPK activation. Furthermore, treatment with an AMPK inhibitor significantly reduced DTMUV production by suppressing viral RNA replication—effects consistent with those observed upon treatment with VSCCs or a cytoplasmic  $\text{Ca}^{2+}$  chelator. These data indicate that cellular  $\text{Ca}^{2+}$  primarily regulates DTMUV replication via activation of the AMPK signaling pathway. This mechanism aligns with findings from studies of other viruses. For example, DEV infection increases cytoplasmic  $\text{Ca}^{2+}$  levels to activate the CaMKK-II-AMPK pathway and induce autophagy of DEFs; blocking this pathway with specific inhibitors significantly suppresses DEV replication (Yin et al., 2018). Similarly, PRRSV promotes its own replication via the same  $\text{Ca}^{2+}$ -CaMKK-II-AMPK-autophagy axis (Manicassamy et al., 2023). Drawing on the rationale of the aforementioned studies, we investigated whether

AMPK activation mediated by elevated cytoplasmic  $\text{Ca}^{2+}$  could induce autophagy in DEFs. We found that the expression level of microtubule-associated protein 1 light chain 3-II (LC3-II) in DEFs was significantly upregulated at 12 h post-infection with DTMUV. Interestingly, treatment of DEFs with BAPTA-AM and Compound C did not significantly alter the LC3-II expression level induced by DTMUV infection (Supplementary Material). Previously, Hu et al. confirmed that DTMUV infection can induce a complete autophagic response in DEFs by demonstrating the degradation dynamics of p62, the turnover of LC3-II throughout the infection cycle, and the formation of autolysosome-like vesicles observed via transmission electron microscopy (TEM) (Hu et al., 2020). In the present study, LC3-II was employed as the sole marker for autophagy detection, and experimental observations were restricted to a single time point at 12 hours post DTMUV infection. As a result, dynamic changes in autophagy throughout the entire course of DTMUV infection could not be fully captured. Thus, the available data are insufficient to elucidate whether autophagy modulates DTMUV replication via the calcium-AMPK signaling pathway, and the underlying molecular mechanisms merit further investigation. In addition, another potential mechanism is associated with oxidative stress, a biological state characterized by the disruption of the balance between the accumulation and clearance of intracellular reactive oxygen species (ROS). Accumulating evidence has confirmed that oxidative stress,  $\text{Ca}^{2+}$  signaling, AMPK activity, and autophagy form a highly interconnected regulatory network (Michalak et al., 2025). Among the Flavivirus genus, such as HCV, DENV, and Japanese encephalitis virus (JEV) have all been shown to induce ROS production, thereby triggering oxidative stress in infected cells (Korenaga et al., 2005; Guzman et al., 2014; Ghoshal et al., 2007). A close bidirectional interaction exists between ROS and  $\text{Ca}^{2+}$  signaling: on the one hand, ROS can modulate intracellular calcium signaling; on the other hand,  $\text{Ca}^{2+}$  signaling is a prerequisite for ROS generation (Görlach et al., 2015). For instance, studies have demonstrated that ROS facilitate calcium ion uptake in vascular smooth muscle cells via L-type and T-type voltage-gated calcium channels (Tabet et al., 2004); conversely,  $\text{Ca}^{2+}$  influx in neutrophils promotes ROS production by activating the recruitment of  $\text{Ca}^{2+}$ -dependent S100A8/A9 proteins (Brécharde et al., 2013). Furthermore, in viral infection models, ROS can promote AMPK activation, thereby regulating autophagy and metabolism-related processes (Zhao et al., 2025). At the level of viral life cycle regulation, oxidative stress has been verified to modulate the capping of flaviviral RNA, which in turn enhances viral proliferation (Gullberg et al., 2015). Taken together, based on existing research findings and the data from the present study, we hypothesize that cellular oxidative stress may be involved in the regulation of viral replication via the  $\text{Ca}^{2+}$ -AMPK axis induced by DTMUV infection, and this hypothesis warrants systematic verification in subsequent studies. Besides, it is worth noting that the  $\text{Ca}^{2+}$ -CAMKK-II axis is not the sole pathway mediating the activation of AMPK during viral infection. As another upstream kinase of AMPK, liver kinase B1 (LKB1) also has the capacity to

activate AMPK. For instance, the NS1 protein of dengue virus type 2 (DENV-2) could act as an assembly scaffold to facilitate the AMPK-LKB1 interaction, thereby inducing AMPK activation (Wu et al., 2023). Therefore, subsequent studies should investigate the role of LKB1 in AMPK activation induced by duck Tembusu virus (DTMUV) infection.

Flaviviruses typically establish an optimal replication environment by comprehensively modulating these metabolic processes of the host. On one hand, flavivirus infection can enhance the glycolytic pathway and pentose phosphate pathway of host cells, a phenomenon observed with viruses such as dengue virus DENV and JEV (Allonso et al., 2015; Li et al., 2021). The glycolysis process promoted by viral infection regulates multiple physiological processes, including increasing the reserves of adenosine triphosphate (ATP) and nucleotides to provide essential energy supply and precursor substances for material synthesis during viral replication. In addition, flavivirus replication requires the formation of invaginated structures on the endoplasmic reticulum membrane, known as replication compartments (RCs) (Gillespie et al., 2010). Flavivirus infection usually reshapes the host membrane system by promoting the synthesis of specific lipids to ensure the complete formation of RCs. For instance, WNV infection recruits 3-hydroxy-3-methylglutaryl-CoA reductase (HMGCR), a key enzyme in cholesterol biosynthesis, to RCs, thereby enhancing cholesterol synthesis and accumulation in the RC region. Inhibition of this process blocks WNV replication (Mackenzie et al., 2007). The non-structural protein 3 (NS3) of DENV relocalizes fatty acid synthase (FASN) to viral replication sites and promotes cellular fatty acid synthesis, thus facilitating the establishment of RCs (Heaton et al., 2010). Intracellular lipid droplets also serve as important targets for host metabolic regulation following flavivirus infection. Early in DENV infection, lipid droplet reabsorption into the endoplasmic reticulum can be observed, a process that may provide lipid raw materials for endoplasmic reticulum expansion and RC formation (Peña and Harris, 2012). In the late stage of infection, DENV induces lipophagy, a type of selective autophagy, through which lipids in lipid droplets are mobilized for  $\beta$ -oxidation and energy production (Heaton and Randall, 2010). As a central regulator of intracellular energy homeostasis, the activated AMPK modulates various cellular metabolic pathways, including lipid homeostasis maintenance and glycolysis, via phosphorylating downstream key targets (Herzig and Shaw, 2017). Based on the aforementioned findings regarding flaviviruses, we postulate that the activation of the AMPK pathway induced by DTMUV infection is likely involved in the reprogramming of host cellular metabolic programs, thereby establishing a favorable intracellular environment for viral replication. Further studies are required to elucidate the detailed molecular mechanism underlying this process.

In summary, our data demonstrate that DTMUV infection significantly disrupts  $\text{Ca}^{2+}$  homeostasis in host cells. Dysregulation of intracellular  $\text{Ca}^{2+}$  homeostasis activates the AMPK signaling pathway, which is a critical prerequisite for DTMUV to complete viral RNA replication. These findings provide a theoretical basis for elucidating the pathogenic mechanism of DTMUV and identifying novel antiviral targets.

## Data availability statement

The original contributions presented in the study are included in the article/Supplementary Material. Further inquiries can be directed to the corresponding authors.

## Author contributions

ZY: Conceptualization, Data curation, Formal analysis, Funding acquisition, Investigation, Methodology, Project administration, Resources, Software, Validation, Visualization, Writing – original draft. XC: Data curation, Investigation, Methodology, Writing – review & editing. WZ: Formal analysis, Funding acquisition, Supervision, Writing – review & editing. ZM: Software, Validation, Writing – review & editing. ZX: Formal analysis, Funding acquisition, Writing – review & editing. KL: Methodology, Software, Writing – review & editing. JW: Data curation, Methodology, Visualization, Writing – review & editing. TL: Data curation, Formal analysis, Writing – review & editing. GZ: Formal analysis, Funding acquisition, Writing – review & editing. BW: Conceptualization, Formal analysis, Writing – review & editing. RX: Formal analysis, Methodology, Writing – review & editing. CL: Formal analysis, Writing – review & editing. HZ: Conceptualization, Funding acquisition, Supervision, Writing – review & editing. JS: Investigation, Methodology, Supervision, Writing – review & editing.

## Funding

The author(s) declared that financial support was received for this work and/or its publication. This research was funded by the following: a 2025 High-Level Talent Research Initiation Fund Project (First Batch) of Wuhu Vocational and Technical University (Grant No. wzyrc202504); Zhang Haiyan Master Studio (Grant No. J20240004), Anhui Province; 2023 Anhui Province University Scientific Research Projects (Grant No. 2023AH052374 and Grant No. 2023AH052397); a 2024 Anhui Province University Scientific Research Project (Grant No. 2024AH052009); National Natural Science Foundation of China (Grant No. 32503029); and a 2025 Annual University-Level Scientific Research Project of Wuhu Vocational and Technical University (Grant No. wzyrzd202511).

## References

- Allonso, D., Andrade, I. S., Conde, J. N., Coelho, D. R., Rocha, D. C., Da Silva, M. L., et al. (2015). Dengue virus NS1 protein modulates cellular energy metabolism by increasing glyceraldehyde-3-phosphate dehydrogenase activity. *J. Virol.* 89, 11871–11883. doi: 10.1128/JVI.01342-15
- Bai, D., Fang, L., Xia, S., Ke, W., Wang, J., Wu, X., et al. (2020). Porcine deltacoronavirus (PDCoV) modulates calcium influx to favor viral replication. *Virology* 539, 38–48. doi: 10.1016/j.virol.2019.10.011
- Balijepalli, R. C., Foell, J. D., Hall, D. D., Hell, J. W., and Kamp, T. J. (2006). Localization of cardiac L-type Ca(2+) channels to a caveolar macromolecular signaling complex is required for beta(2)-adrenergic regulation. *Proc. Natl. Acad. Sci. U.S.A.* 103, 7500–7505. doi: 10.1073/pnas.0503465103
- Berridge, M. J., Bootman, M. D., and Roderick, H. L. (2003). Calcium signalling: dynamics, homeostasis and remodelling. *Nat. Rev. Mol. Cell Biol.* 4, 517–529. doi: 10.1038/nrm1155
- Berridge, M. J., Lipp, P., and Bootman, M. D. (2000). The versatility and universality of calcium signalling. *Nat. Rev. Mol. Cell Biol.* 1, 11–21. doi: 10.1038/35036035
- Bezemer, B., Van Cleef, K. W. R., Overheul, G. J., Miesen, P., and Van Rij, R. P. (2022). The calcium channel inhibitor lacidipine inhibits Zika virus replication in neural progenitor cells. *Antiviral Res.* 202, 105313. doi: 10.1016/j.antiviral.2022.105313
- Bréchar, S., Plançon, S., and Tschirhart, E. J. (2013). New insights into the regulation of neutrophil NADPH oxidase activity in the phagosome: a focus on the role of lipid and Ca (2+) signaling. *Antioxid Redox Signal* 18, 661–676. doi: 10.1089/ars.2012.4773
- Casciano, J. C., and Bouchard, M. J. (2018). Hepatitis B virus X protein modulates cytosolic Ca2+ signaling in primary human hepatocytes. *Virus Res.* 246, 23–27. doi: 10.1016/j.virusres.2018.01.001
- Chen, F., Shen, H., Liu, G., Zhang, P., Zhang, L., Lin, S., et al. (2024). Verapamil inhibits respiratory syncytial virus infection by regulating Ca2+ influx. *Life Sci.* 352, 122877. doi: 10.1016/j.lfs.2024.122877

## Acknowledgments

We thank Michelle Kahmeyer-Gabbe, PhD, from Liwen Bianji (Edanz) ([www.liwenbianji.cn](http://www.liwenbianji.cn)) for editing the English text of a draft of this manuscript.

## Conflict of interest

The author(s) declared that this work was conducted in the absence of any commercial or financial relationships that could be construed as a potential conflict of interest.

## Generative AI statement

The author(s) declared that generative AI was not used in the creation of this manuscript.

Any alternative text (alt text) provided alongside figures in this article has been generated by Frontiers with the support of artificial intelligence and reasonable efforts have been made to ensure accuracy, including review by the authors wherever possible. If you identify any issues, please contact us.

## Publisher's note

All claims expressed in this article are solely those of the authors and do not necessarily represent those of their affiliated organizations, or those of the publisher, the editors and the reviewers. Any product that may be evaluated in this article, or claim that may be made by its manufacturer, is not guaranteed or endorsed by the publisher.

## Supplementary material

The Supplementary Material for this article can be found online at: <https://www.frontiersin.org/articles/10.3389/fcimb.2026.1743907/full#supplementary-material>

- Cheshenko, N., Del Rosario, B., Woda, C., Marcellino, D., Satlin, L. M., and Herold, B. C. (2003). Herpes simplex virus triggers activation of calcium-signaling pathways. *J. Cell Biol.* 163, 283–293. doi: 10.1083/jcb.200301084
- Ding, W., Albrecht, B. R., Kelley, R. E., Muthusamy, N., Kim, S.-J., Altschuld, R. A., et al. (2002). Human T-cell lymphotropic virus type 1 p12IExpression increases cytoplasmic calcium to enhance the activation of nuclear factor of activated T cells. *J. Virol.* 76, 10374–10382. doi: 10.1128/JVI.76.20.10374-10382.2002
- Dionicio, C. L., Peña, F., Constantino-Jonapa, L. A., Vazquez, C., Yocupicio-Monroy, M., Rosales, R., et al. (2018). Dengue virus induced changes in Ca<sup>2+</sup> homeostasis in human hepatic cells that favor the viral replicative cycle. *Virus Res.* 245, 17–28. doi: 10.1016/j.virusres.2017.11.029
- Fujioka, Y., Nishide, S., Ose, T., Suzuki, T., Kato, I., Fukuhara, H., et al. (2018). A sialylated voltage-dependent Ca<sup>2+</sup> Channel binds hemagglutinin and mediates influenza A virus entry into mammalian cells. *Cell Host Microbe* 23, 809–818.e5. doi: 10.1016/j.chom.2018.04.015
- Ghoshal, A., Das, S., Ghosh, S., Mishra, M. K., Sharma, V., Koli, P., et al. (2007). Proinflammatory mediators released by activated microglia induces neuronal death in Japanese encephalitis. *Glia* 55, 483–496. doi: 10.1002/glia.20474
- Gillespie, L. K., Hoenen, A., Morgan, G., and Mackenzie, J. M. (2010). The endoplasmic reticulum provides the membrane platform for biogenesis of the flavivirus replication complex. *J. Virol.* 84, 10438–10447. doi: 10.1128/JVI.00986-10
- Görlach, A., Bertram, K., Hudecova, S., and Krizanova, O. (2015). Calcium and ROS: A mutual interplay. *Redox Biol.* 6, 260–271. doi: 10.1016/j.redox.2015.08.010
- Griffin, S. D. C., Beales, L. P., Clarke, D. S., Worsfold, O., Evans, S. D., Jaeger, J., et al. (2002). The p7 protein of hepatitis C virus forms an ion channel that is blocked by the antiviral drug, Amantadine. *FEBS Lett.* 535, 34–38. doi: 10.1016/S0014-5793(02)03851-6
- Gu, Y., Qi, B., Zhou, Y., Jiang, X., Zhang, X., Li, X., et al. (2016). Porcine circovirus type 2 activates CaMKK $\beta$  to initiate autophagy in PK-15 cells by increasing cytosolic calcium. *Viruses* 8, 135. doi: 10.3390/v8050135
- Gullberg, R. C., Jordan Steel, J., Moon, S. L., Soltani, E., and Geiss, B. J. (2015). Oxidative stress influences positive strand RNA virus genome synthesis and capping. *Virology* 475, 219–229. doi: 10.1016/j.virol.2014.10.037
- Guzman, M. G., Al-Alimi, A. A., Ali, S. A., Al-Hassan, F. M., Idris, F. M., Teow, S.-Y., et al. (2014). Dengue virus nonstructural protein 3 redistributes fatty acid synthase to sites of viral replication and increases cellular fatty acid synthesis. *Proc. Natl. Acad. Sci. U.S.A.* 111, 17345–17350. doi: 10.1073/pnas.1010811117
- Heaton, N. S., Perera, R., Berger, K. L., Khadka, S., Lacount, D. J., Kuhn, R. J., et al. (2010). Dengue virus nonstructural protein 3 redistributes fatty acid synthase to sites of viral replication and increases cellular fatty acid synthesis. *Proc. Natl. Acad. Sci. U.S.A.* 107, 17345–17350. doi: 10.1073/pnas.1010811117
- Heaton, N. S., and Randall, G. (2010). Dengue virus-induced autophagy regulates lipid metabolism. *Cell Host Microbe* 8, 422–432. doi: 10.1016/j.chom.2010.10.006
- Herzig, S., and Shaw, R. J. (2017). AMPK: guardian of metabolism and mitochondrial homeostasis. *Nat. Rev. Mol. Cell Biol.* 19, 121–135. doi: 10.1038/nrm.2017.95
- Homonnay, Z. G., Kovács, E. W., Bányai, K., Albert, M., Fehér, E., Mató, T., et al. (2014). Tembusu-like flavivirus (Perak virus) as the cause of neurological disease outbreaks in young Pekin ducks. *Avian Pathol.* 43, 552–560. doi: 10.1080/03079457.2014.973832
- Hu, Z., Pan, Y., Cheng, A., Zhang, X., Wang, M., Chen, S., et al. (2020). Autophagy promotes duck tembusu virus replication by suppressing p62/SQSTM1-mediated innate immune responses *in vitro*. *Vaccines* 8, 22. doi: 10.3390/vaccines8010022
- Korenaga, M., Wang, T., Li, Y., Showalter, L. A., Chan, T., Sun, J., et al. (2005). Hepatitis C virus core protein inhibits mitochondrial electron transport and increases reactive oxygen species (ROS) production. *J. Biol. Chem.* 280, 37481–37488. doi: 10.1074/jbc.M506412200
- Lee, B., Qu, Y., Wang, S., Jiang, H., Liao, Y., Qiu, X., et al. (2024). Newcastle disease virus infection induces parthanatos in tumor cells via calcium waves. *PLoS Pathog.* 20, e1012737. doi: 10.1371/journal.ppat.1012737
- Li, M., Yang, J., Ye, C., Bian, P., Yang, X., Zhang, H., et al. (2021). Integrated metabolomics and transcriptomics analyses reveal metabolic landscape in neuronal cells during JEV infection. *Virol. Sin.* 36, 1554–1565. doi: 10.1007/s12250-021-00445-0
- Mackenzie, J. M., Khromykh, A. A., and Parton, R. G. (2007). Cholesterol manipulation by West Nile virus perturbs the cellular immune response. *Cell Host Microbe* 2, 229–239. doi: 10.1016/j.chom.2007.09.003
- Manicassamy, B., Diao, F., Jiang, C., Sun, Y., Gao, Y., Bai, J., et al. (2023). Porcine reproductive and respiratory syndrome virus infection triggers autophagy via ER stress-induced calcium signaling to facilitate virus replication. *PLoS Pathog.* 19, e1011295. doi: 10.1371/journal.ppat.1011295
- Michalak, K. P., Michalak, A. Z., and Brenk-Krakowska, A. (2025). Acute COVID-19 and LongCOVID syndrome – molecular implications for therapeutic strategies - review. *Front. Immunol.* 16. doi: 10.3389/fimmu.2025.1582783
- Ninvilai, P., Nonthabenjawan, N., Limcharoen, B., Tunterak, W., Oraveerakul, K., Banlunara, W., et al. (2018). The presence of duck Tembusu virus in Thailand since 2007: A retrospective study. *Transboundary Emerging Dis.* 65, 1208–1216. doi: 10.1111/tbed.12859
- Osuna-Ramos, J. F., Reyes-Ruiz, J. M., and Del Ángel, R. M. (2018). The role of host cholesterol during flavivirus infection. *Front. Cell. Infection Microbiol.* 8. doi: 10.3389/fcimb.2018.00388
- Pani, B., and Singh, B. B. (2009). Lipid rafts/caveolae as microdomains of calcium signaling. *Cell Calcium* 45, 625–633. doi: 10.1016/j.ceca.2009.02.009
- Peña, J., and Harris, E. (2012). Early dengue virus protein synthesis induces extensive rearrangement of the endoplasmic reticulum independent of the UPR and SREBP-2 pathway. *PLoS One* 7, e38202. doi: 10.1371/journal.pone.0038202
- Platt, G. S., Way, H. J., Bowen, E. T. W., Simpson, D. I. H., Hill, M. N., Kamath, S., et al. (2016). Arbovirus infections in Sarawak, October 1968–February 1970 Tembusu and Sindbis virus isolations from mosquitoes. *Ann. Trop. Med. Parasitol.* 69, 65–71. doi: 10.1080/00034983.1975.11686984
- Qiu, J., Su, J., Li, S., Hu, X., Yu, X., Wang, Y., et al. (2011). Duck egg-drop syndrome caused by BYD virus, a new tembusu-related flavivirus. *PLoS One* 6, e18106. doi: 10.1371/journal.pone.0018106
- Salt, I., Carling, D., Mcaloon, L. M., Muller, A. G., Nay, K., Lu, E. L., et al. (2024). CaMKK2: bridging the gap between Ca<sup>2+</sup> signaling and energy-sensing. *Essays Biochem.* 68, 309–320. doi: 10.1042/EBC20240011
- Scherbik, S. V., and Brinton, M. A. (2010). Virus-induced Ca<sup>2+</sup> influx extends survival of west Nile virus-infected cells. *J. Virol.* 84, 8721–8731. doi: 10.1128/JVI.00144-10
- Tabet, F., Savoia, C., Schiffrin, E. L., and Touyz, R. M. (2004). Differential calcium regulation by hydrogen peroxide and superoxide in vascular smooth muscle cells from spontaneously hypertensive rats. *J. Cardiovasc. Pharmacol.* 44, 200–208. doi: 10.1097/00005344-200408000-00009
- Tang, Y., Diao, Y., Gao, X., Yu, C., Chen, L., and Zhang, D. (2012). Analysis of the complete genome of tembusu virus, a flavivirus isolated from ducks in China. *Transboundary Emerging Dis.* 59, 336–343. doi: 10.1111/j.1865-1682.2011.01275.x
- Tokumitsu, H., and Sakagami, H. (2022). Molecular mechanisms underlying Ca<sup>2+</sup>/calmodulin-dependent protein kinase kinase signal transduction. *Int. J. Mol. Sci.* 23, 11025. doi: 10.3390/ijms231911025
- Wu, N., Ji, J., Gou, X., Hu, P., Cheng, Y., Liu, Y., et al. (2023). DENV-2 NS1 promotes AMPK-LKB1 interaction to activate AMPK/ERK/mTOR signaling pathway to induce autophagy. *Virol. J.* 20, 231. doi: 10.1186/s12985-023-02166-0
- Yan, D., Li, X., Wang, Z., Liu, X., Dong, X., Fu, R., et al. (2022). The emergence of a disease caused by a mosquito origin Cluster 3.2 Tembusu virus in chickens in China. *Veterinary Microbiol.* 272, 109500. doi: 10.1016/j.vetmic.2022.109500
- Yin, H., Zhao, L., Wang, Y., Li, S., Huo, H., and Chen, H. (2018). Duck enteritis virus activates CaMKK $\beta$ -AMPK to trigger autophagy in duck embryo fibroblast cells via increased cytosolic calcium. *Virol. J.* 15, 120. doi: 10.1186/s12985-018-1029-0
- Yu, Z., Ren, H., Sun, M., Xie, W., Sun, S., Liang, N., et al. (2021). Tembusu virus infection in laying chickens: Evidence for a distinct genetic cluster with significant antigenic variation. *Transboundary Emerging Dis.* 69, e1130–e1141. doi: 10.1111/tbed.14402
- Zhang, P., Fu, H.-J., Lv, L.-X., Liu, C.-F., Han, C., Zhao, X.-F., et al. (2023). WSSV exploits AMPK to activate mTORC2 signaling for proliferation by enhancing aerobic glycolysis. *Commun. Biol.* 6, 361. doi: 10.1038/s42003-023-04735-z
- Zhao, Y., Qi, X., Zhu, Z., Wang, W., Wen, W., and Li, X. (2025). Increased ROS levels activate AMPK-ULK1-mediated mitophagy to promote pseudorabies virus replication. *Vet. Res.* 56, 156. doi: 10.1186/s13567-025-01595-9
- Zhou, Y., Frey, T. K., and Yang, J. J. (2009). Viral calciomics: Interplays between Ca<sup>2+</sup> and virus. *Cell Calcium* 46, 1–17. doi: 10.1016/j.ceca.2009.05.005